Disturbance scaling in bidirectional vehicle platoons with different asymmetry in position and velocity coupling

Ivo Herman [a], Steffi Knorn [b] and Anders Ahlén [b]

[a] *Department of Control Engineering, Czech Technical University in Prague, Prague, Czech Republic*

[b] *Signals and Systems, Uppsala University, Sweden*

Abstract

This paper considers a string of vehicles where the local control law uses the states of the vehicle's immediate predecessor and follower. The coupling towards the preceding vehicle can be chosen different to the coupling with the following vehicle, which is referred to as an asymmetric bidirectional string. Further, the asymmetry for the velocity coupling can be chosen differently to the asymmetry in the position coupling. It is investigated how the effect of the disturbance on the control errors in the string depends on the string length. It is shown, that in case of symmetric position coupling and asymmetric velocity coupling, linear scaling can be achieved. For symmetric interactions, the errors scale quadratically in the number of vehicles. When the coupling in position is asymmetric, exponential scaling may occur or the system might even become unstable. The paper thus gives a comprehensive overview of the achievable performance in linear, asymmetric, bidirectional platoons. The results reveal that symmetry in the position coupling and asymmetry in velocity coupling qualitatively improves the performance of the string. Extensive numerical results illustrate the theoretical findings.

Key words: Port-Hamiltonian Systems, Vehicular platoons, Multi-Vehicle Systems, Scaling, Asymmetry

1 Introduction

Vehicle platoons are anticipated to increase both the safety and capacity of highways. In its simplest form, a platoon, consisting of N cooperatively-acting, automatically controlled vehicles, travels in a longitudinal line with tight spacing between the vehicles. An important safety and performance measure in this area is how the response of the platoon to disturbances scales with respect to N. When the local errors are bounded independently of N, the string is "string stable". Generally speaking, a platoon is string stable if disturbances propagating through the string do not grow with N or the position within the string, Ploeg et al. (2014).

The literature often distinguishes between "unidirectional" strings, where each vehicle only considers information of a group of direct predecessors, and "bidirectional", where information from following vehicles is also used. A strict form of string stability in linear vehicle strings with double integrators in the open loop, local information only and tight spacing, can neither be achieved in unidirectional nor in bidirectional strings, Seiler et al. (2004), Barooah & Hespanha (2005). This definition of string stability requires the L_2 norm of the local error vector to be bounded for any L_2 bounded disturbance vector. In unidirectional strings, string stability can be achieved using a time headway spacing policy, Klinge & Middleton (2009), Middleton & Braslavsky (2010), or inter-vehicle communication, Alam et al. (2015). However, the time-headway policy leads to undesirable large steady-state inter vehicle distances and wireless communication between the vehicles can potentially be disturbed by an intruder.

Bidirectional strings seem to offer advantages, as also backward distance errors are used to control the vehicle. If the the forward distance error is weighed equally to the backward distance error, the string is referred to as a "symmetric". By Knorn et al. (2014) a weaker form of string stability can be achieved, where the L_∞ norm of the local error vector is guaranteed to be bounded for any disturbances in L_2. The results were extended by Knorn et al. (2015) and Knorn & Ahlén (2016). In contrast, by weighing the forward error higher, that is, allowing asymmetric controller gains, a uniform bound on the eigenvalues of the formation can be achieved, see Hao & Barooah (2012), which guarantees faster transients compared to symmetric control.

The drawback of the better convergence rate is exponential scaling in N of the $\mathcal{H}_\infty$ norm of the transfer functions for asymmetric strings compared to linear scaling for symmetric strings, see Veerman et al. (2007). This was first shown

Email addresses: ivo.herman@fel.cvut.cz (Ivo Herman), steffi.knorn@signal.uu.se (Steffi Knorn), anders.ahlen@signal.uu.se (Anders Ahlén).

[1] The research of Ivo Herman was supported by the Czech Science Foundation within the project GACR 16-19526S.

for a double-integrator model by Tangerman et al. (2012) and later generalized by Herman et al. (2015) and Herman, Martinec, Hurák & Sebek (2016).

Many works in the area assume that the degree of asymmetry in the position and velocity coupling is identical, e. g. Barooah et al. (2009). But the performance of the string can be improved by allowing symmetric position coupling and asymmetric velocity coupling. Good stability margin properties were shown by Hao & Barooah (2010). A good scaling of system norms with such an approach was numerically shown in Hao et al. (2012) and the properties of the platoon's response to a step change in leader's velocity were derived by Cantos et al. (2016). Using these properties, the parameters of the controller as well as the coefficient of asymmetry can be optimised to minimise the transient time, see Herman, Martinec & Veerman (2016). In both papers by Cantos et al. (2016), Herman, Martinec & Veerman (2016) it was shown that symmetry in position is necessary for a good scaling. In addition, it was proved by Martinec et al. (2016) that symmetry in position is a necessary condition for "local" string stability.

1.1 Problem formulation

This paper considers a heterogeneous, asymmetric, bidirectional string of N vehicles with constant masses m_i, positions x_i, velocities v_i and momenta p_i for all $i \in \{1, 2, \dots, N\}$. The vehicles are modelled as double integrators such that

$$m_i \ddot{x}_i = F_i + d_i, \tag{1}$$

where d_i is the disturbance acting on vehicle i. The linear control force F_i has the form

$$\begin{aligned} F_i =& (1 + h_\mathrm{p}) r_i (v_{i-1} - v_i) - (1 - h_\mathrm{p}) r_{i+1} (v_i - v_{i+1}) \\ &+ (1 + h_\Delta) a_i \Delta_i - (1 - h_\Delta) a_{i+1} \Delta_{i+1}, \end{aligned} \tag{2}$$

where $\Delta_i := x_{i-1} - x_i - \delta_{\mathrm{ref}\,i-1,i}$ is the local position error between vehicle i and its predecessor $i-1$, aimed to be kept at the fixed distance $\delta_{\mathrm{ref}\,i-1,i}$; constants $r_i > 0$ and $a_i > 0$ are the velocity and position coupling parameters and h_p and h_Δ are the asymmetry coefficients for the velocity and position coupling, respectively. The index $i = 0$ refers to a virtual reference vehicle with position x_0, velocity v_0 and momenta p_0 and the last vehicle only considers the forward error.

This paper investigates the disturbance scaling for such asymmetric bidirectional platoons.

Definition 1 *Collecting all error states of the platoon in the vector $\chi(t)$ and all disturbances in the vector $d(t)$,* disturbance scaling *refers to how the scaling factor ξ in $|\chi(t)| \leq |\chi(0)| + \xi \|d(\cdot)\|_2$ scales with the string length N, where $\|d(\cdot)\|_2$ denotes the L_2 norm of the disturbances.*

1.2 Contributions

Figure 1 summarises how ξ scales with N for different choices of h_p and h_Δ. The point $h_\mathrm{p} = h_\Delta = 0$ corresponds to the symmetric, bidirectional case while $h_\mathrm{p} = h_\Delta = 1$ describes the unidirectional ("predecessor following" = 'PF') case. The findings can be summarised as follows:

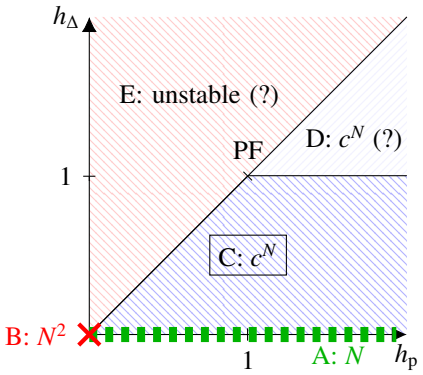

Figure 1. Disturbance scaling with respect to N for different selections of asymmetry. Area A: linear scaling, Area B: quadratic, Area C and D: exponential. Conjectures are marked with (?).

(1) It is shown that asymmetry in velocity with symmetric position coupling, i.e., case A, achieves linear scaling, while a completely symmetric control scales quadratically, i.e., case B. See Section 3. [2]

(2) It is shown that for asymmetric position coupling below a certain bound, the errors scale exponentially, i.e., case C, see Section 4.1. We conjecture that it is also true for $h_\Delta \geq 1$, i.e., case D.

(3) It is shown that for some cases of stronger asymmetry in the position coupling compared to the velocity coupling, i.e., for a subset of case E, the system is unstable for a sufficiently high N, see Section 4.2. We conjecture that for all strings in E a finite critical N, which is the maximal stable string length, exists.

(4) Extensive numerical results are presented to illustrate the technical results, see Section 5.

(5) The system description unifies several existing platoon descriptions such as unidirectional strings, Seiler et al. (2004), bidirectional symmetric strings, Knorn et al. (2014), Barooah & Hespanha (2005), and bidirectional asymmetric strings, e. g. Barooah et al. (2009), Cantos et al. (2016).

Notation: The L_2 vector norm is $|x|_2^2 = x^\mathrm{T} x$ and the L_2 vector norm $\|x(\cdot)\|_2^2 = \int_0^\infty |x(t)|_2^2 \mathrm{d}t$. For a scalar function $H(x)$ of a vector $x = [x_1, \dots, x_n]^\mathrm{T}$ its gradient is defined as $\nabla H(x) = \left[\frac{\partial H(x)}{\partial x_1}, \frac{\partial H(x)}{\partial x_2}, \dots, \frac{\partial H(x)}{\partial x_n}\right]^\mathrm{T}$ and its ith element $\nabla_{x_i} H(x)$. $x(t) = \mathrm{col}(x_1(t), \dots, x_N(t))$ is the column vector with N elements. The column vector of ones of length N is $\underline{1}$. Denote the diagonal matrix $A \in \mathbb{R}^{N \times N}$ with diagonal entries $a_1, \dots a_N$ as $A = \mathrm{diag}(a_1, \dots a_N)$. The matrix $\langle A \rangle$ is a matrix obtained from A by taking the absolute values of the elements. $A > 0$ and $A \geq 0$ denote that A is a positive definite or positive semi-definite matrix, respectively. $\sigma_i(A)$ is the ith smallest singular value of A and $\lambda_i(A)$ is the ith small-

[2] To the best knowledge of the authors, this is the first paper which analytically proves better scaling when symmetry in position and asymmetry in velocity is used. The papers by Cantos et al. (2016), Herman, Martinec & Veerman (2016) relied in their proofs only on (reasonable, though) conjectures.

est eigenvalue. $\sigma_{\min}(A)$, $\sigma_{\max}(A)$ ($\lambda_{\min}(A), \lambda_{\max}(A)$) are the minimal and maximal singular values (eigenvalues) of A.

2 Mathematical preliminaries

Consider the dynamics in (1) and (2) with constant, bounded control parameters and vehicle masses:

Assumption 2 *There exist constants* $\underline{r} > 0$, $\overline{r} < \infty$, $\underline{m} > 0, \overline{m} < \infty$, $\underline{a} > 0, \overline{a} < \infty$ *such that* $\underline{r} \le r_i \le \overline{r}$, $\underline{m} \le m_i \le \overline{m}$ *and* $\underline{a} \le a_i \le \overline{a}$ *for all* $i \le N$ *and for all* N.

By collecting the positions in $x(t) = \mathrm{col}(x_1, \dots, x_N)$, and introducing $\delta_{\mathrm{ref}} = \mathrm{col}(\delta_{\mathrm{ref}0,1}, \dots, \delta_{\mathrm{ref}0,N})$ the local position errors can be represented by $\Delta(t) := \mathrm{col}(\Delta_1, \dots, \Delta_N) = -\mathcal{B}^{\mathrm{T}}(x(t) - \underline{1}x_0(t) + \delta_{\mathrm{ref}})$, where the coupling matrix $\mathcal{B}$ is

$$\mathcal{B} = \begin{bmatrix} 1 & -1 & 0 & \cdots & 0 \\ 0 & \ddots & \ddots & \ddots & 0 \\ \vdots & & \ddots & 1 & -1 \\ 0 & \cdots & 0 & 0 & 1 \end{bmatrix}. \tag{3}$$

Let $R = \mathrm{diag}(r_1, \dots, r_N) > 0$ be the matrix of damping coefficients and $M = \mathrm{diag}(m_1, \dots, m_N) > 0$ be the inertia matrix. Further, let the velocity asymmetry matrix be given as $\tilde{\mathcal{B}}_{\mathrm{p}} = h_{\mathrm{p}}\langle\mathcal{B}\rangle$. Then the vector of forces due to relative velocities is described by $F^{\mathrm{r}} = -(\mathcal{B} + \tilde{\mathcal{B}}_{\mathrm{p}})R\mathcal{B}^{\mathrm{T}}(M^{-1}p - \underline{1}v_0)$, where $p = \mathrm{col}(p_1, \dots, p_N)$ is the momentum vector. The vector of forces due to position errors can be written as $F^{\mathrm{s}} = (\mathcal{B} + \tilde{\mathcal{B}}_{\Delta})A\Delta$, where $A = \mathrm{diag}(a_1, \dots a_N) > 0$ and $\tilde{\mathcal{B}}_{\Delta} = h_{\Delta}\langle\mathcal{B}\rangle$. Hence, $F = \mathrm{col}(F_1, \dots, F_N) = F^{\mathrm{r}} + F^{\mathrm{s}}$.

We will analyse the following asymmetry combinations:

- $h_{\Delta} = 0, h_{\mathrm{p}} = 0$, which refers to symmetric position and symmetric velocity coupling, abbreviated as *SPSV*.
- $h_{\Delta} = 0, h_{\mathrm{p}} > 0$, which refers to symmetric position and asymmetric velocity coupling, abbreviated as *SPAV*.
- $h_{\Delta} > 0, h_{\mathrm{p}} \ge 0$, which refers to asymmetric position and asymmetric velocity coupling, abbreviated as *APAV*.

3 Symmetric position coupling

This section considers symmetric position forces, such that the platoon can be written in the port-Hamiltonian form

$$\begin{bmatrix} \dot{p}(t) \\ \dot{\Delta}(t) \end{bmatrix} = \begin{bmatrix} -(\mathcal{B} + \tilde{\mathcal{B}}_{\mathrm{p}})R\mathcal{B}^{\mathrm{T}} & \mathcal{B} \\ -\mathcal{B}^{\mathrm{T}} & 0 \end{bmatrix} \nabla H(p(t), \Delta(t)) + \begin{pmatrix} d(t) \\ 0 \end{pmatrix}, \tag{4}$$

with $h_{\Delta} = 0$ (and thus $\tilde{\mathcal{B}}_{\Delta} = 0$) and the Hamiltonian function

$$H(p, \Delta) = \frac{1}{2}(p(t) - M\underline{1}v_0)^{\mathrm{T}}M^{-1}(p(t) - M\underline{1}v_0) + \frac{1}{2}\Delta^{\mathrm{T}}(t)A\Delta(t) \tag{5}$$

and the equilibrium

$$\Delta_i = 0 \text{ and } v_i = v_0 \text{ for all } i \le N. \tag{6}$$

The Hamiltonian $H(p, \Delta)$ captures the kinetic "energy" stored in the relative velocity to the leader and potential "energy" stored in the position errors. Hence, it captures both the spacing and velocity errors of all vehicles. In the following we provide an upper bound on the Hamiltonian, leading to a bound on the maximal error.

The following assumption is necessary to guarantee, that (5) is a suitable Hamiltonian function for SPAV systems.

Assumption 3 $r_i \ge r_{i+1}$ *for all* $i < N$.

SPSV and SPAV systems have similar properties:

Theorem 4 (SPSV, SPAV) *Consider system* (4), (5) *under Assumption 2. If* $h_{\mathrm{p}} > 0$ *(SPAV), the following holds under Assumption 3; if* $h_{\mathrm{p}} = 0$ *(SPSV), it holds unconditionally:*

(i) for $d(t) \equiv 0$ *the equilibrium* (6) *of the autonomous system is asymptotically stable,*

(ii) the system is passive with input vector $d(t)$*, output vector* $\nabla_{\mathrm{p}}H$ *and storage function* (5)*,*

(iii) the following bound on the Hamiltonian at time t holds

$$H(p(t), \Delta(t)) \le H(p(0), \Delta(0)) + \frac{\|d(\cdot)\|_2^2}{2\sigma_{\min}\left((\mathcal{B} + h_{\mathrm{p}}\langle\mathcal{B}\rangle)R\mathcal{B}^{\mathrm{T}}\right)}. \tag{7}$$

PROOF. The proof for $h_{\mathrm{p}} = 0$ is found in Knorn & Ahlén (2016). Thus, only the proof for $h_{\mathrm{p}} > 0$ is presented here.

(i) Take H in (5) as a Lyapunov function and set $d(t) = 0$. Then, $\dot{H} = -\nabla_{\mathrm{p}}^{\mathrm{T}}H\left(\mathcal{B} + \tilde{\mathcal{B}}_{\mathrm{p}}\right)R\mathcal{B}^{\mathrm{T}}\nabla_{\mathrm{p}}H$. In order to show that $\dot{H} < 0$, let $\tilde{v}_i$ be the ith element of $\nabla_{\mathrm{p}}H$. Then, since $\left(\mathcal{B} + \tilde{\mathcal{B}}_{\mathrm{p}}\right)R\mathcal{B}^{\mathrm{T}}$ has the tridiagonal structure

$$\begin{bmatrix} (1+h_{\mathrm{p}})r_1 + (1-h_{\mathrm{p}})r_2 & -(1-h_{\mathrm{p}})r_2 & & 0 \\ -(1+h_{\mathrm{p}})r_2 & \ddots & \ddots & \\ & \ddots & \ddots & -(1-h_{\mathrm{p}})r_N \\ 0 & & -(1+h_{\mathrm{p}})r_N & (1+h_{\mathrm{p}})r_N \end{bmatrix},$$

it follows that

$$\begin{aligned} & -\nabla_{\mathrm{p}}^{\mathrm{T}}H(\mathcal{B} + \tilde{\mathcal{B}}_{\mathrm{p}})R\mathcal{B}^{\mathrm{T}}\nabla_{\mathrm{p}}H \\ = & -\left(r_1(1+h_{\mathrm{p}}) + r_2(1-h_{\mathrm{p}})\right)\tilde{v}_1^2 + r_2(1-h_{\mathrm{p}})\tilde{v}_1\tilde{v}_2 \\ & + r_2(1+h_{\mathrm{p}})\tilde{v}_2\tilde{v}_1 - \left(r_2(1+h_{\mathrm{p}}) + r_3(1-h_{\mathrm{p}})\right)\tilde{v}_2^2 + \dots \\ & - r_N(1+h_{\mathrm{p}})\tilde{v}_N^2 \\ \le & -r_1\tilde{v}_1^2 - r_2(\tilde{v}_1 - \tilde{v}_2)^2 - r_3(\tilde{v}_2 - \tilde{v}_3)^2 - \dots \\ & - r_{N-1}(\tilde{v}_{N-1} - \tilde{v}_N)^2 - r_N h_{\mathrm{p}}\tilde{v}_N^2 < 0, \end{aligned}$$

where in the first inequality we used Assumption 3. Hence, the system is Lyapunov stable. Asymptotic stability follows using the invariance principle, see Khalil (2001). The set when $\dot{H} = 0$ is $\nabla_{\mathrm{p}}H = 0$. Then in (4) $\dot{p} = 0 \Leftrightarrow \mathcal{B}\nabla_{\Delta}H = 0$. Since $\nabla_{\Delta}H = A\Delta$ and A and $\mathcal{B}$ are nonsingular, it follows that the only positively invariant set is $\Delta = 0$.

(ii) Considering $d(t)$, the derivative of the Lyapunov function (5) is $\dot{H} = -\nabla_{\mathrm{p}}^{\mathrm{T}}H\left(\mathcal{B} + \tilde{\mathcal{B}}_{\mathrm{p}}\right)R\mathcal{B}^{\mathrm{T}}\nabla_{\mathrm{p}}H + \nabla_{\mathrm{p}}^{\mathrm{T}}Hd(t)$.

Taking $y = \nabla_{\mathrm{p}} H$ as an output yields

$$\dot{H} \leq -\sigma_{\min}\left(\left(\mathcal{B}+\tilde{\mathcal{B}}_{\mathrm{p}}\right) R\mathcal{B}^{\mathrm{T}}\right)|y|_2^2 + y^{\mathrm{T}} d. \tag{8}$$

(iii) Extending (8) by completing the squares leads to

$$\begin{aligned}\dot{H} \leq & -\frac{\sigma_{\min}\left(\left(\mathcal{B}+\tilde{\mathcal{B}}_{\mathrm{p}}\right) R\mathcal{B}^{\mathrm{T}}\right)}{2}|y|_2^2 + \frac{|d(t)|_2^2}{2\sigma_{\min}\left(\left(\mathcal{B}+\tilde{\mathcal{B}}_{\mathrm{p}}\right) R\mathcal{B}^{\mathrm{T}}\right)} \\ & - \frac{\sigma_{\min}\left(\left(\mathcal{B}+\tilde{\mathcal{B}}_{\mathrm{p}}\right) R\mathcal{B}^{\mathrm{T}}\right)}{2}\left|y - \frac{d(t)}{\sigma_{\min}\left(\left(\mathcal{B}+\tilde{\mathcal{B}}_{\mathrm{p}}\right) R\mathcal{B}^{\mathrm{T}}\right)}\right|_2^2 \\ \leq & \frac{1}{2\sigma_{\min}\left(\left(\mathcal{B}+\tilde{\mathcal{B}}_{\mathrm{p}}\right) R\mathcal{B}^{\mathrm{T}}\right)}|d(t)|_2^2. \end{aligned} \tag{9}$$

Integrating with respect to t yields (7). □

3.1 Scaling of singular values

Suppose that the norm of the disturbance signal is fixed for any N. Then, the effect of the disturbance depends on $\sigma_{\min}(\mathcal{B} + h_{\mathrm{p}}\langle\mathcal{B}\rangle)R\mathcal{B}^{\mathrm{T}}$. The smaller it is, the larger will be the effect of the disturbance $d(t)$ on the deviations from the equilibrium. The worst-case convergence rate (8) also depends on this singular value. Below, we will investigate how the smallest singular value scales with N. First, we consider the lower bound. For the proof see Appendix A.

Lemma 5 *Let* $\gamma = \min\{1, 1/h_{\mathrm{p}}\}$. *Then,*

$$\sigma_{\min}\left((\mathcal{B} + h_{\mathrm{p}}\langle\mathcal{B}\rangle)R\mathcal{B}^{\mathrm{T}}\right) \geq \underline{r}\sqrt{1/(16N^4) + h_{\mathrm{p}}^2\gamma/N^2}. \tag{10}$$

The final scaling result, proven in Appendix B, is as follows.

Lemma 6 *With* $c_1, c_2, c_3, c_4 > 0$ *and for N sufficiently large,*

$$\frac{c_1\,\underline{r}}{N} \leq \sigma_{\min}\left(\left(\mathcal{B}+h_{\mathrm{p}}\langle\mathcal{B}\rangle\right)R\mathcal{B}^{\mathrm{T}}\right) \leq \frac{c_2\,\overline{r}}{N} \quad \text{if } h_{\mathrm{p}} > 0, \tag{11}$$

$$\frac{c_3\,\underline{r}}{N^2} \leq \sigma_{\min}\left(\left(\mathcal{B}+h_{\mathrm{p}}\langle\mathcal{B}\rangle\right)R\mathcal{B}^{\mathrm{T}}\right) \leq \frac{c_4\,\overline{r}}{N^2} \quad \text{if } h_{\mathrm{p}} = 0. \tag{12}$$

The upper and lower bounds on $\sigma_{\min}$ are of the same order and approach zero as N grows both for SPAV and SPSV. The rate of approach is quadratic for SPSV, while it is linear for SPAV. Thus, in SPAV systems, the effect of the disturbance is qualitatively smaller than in SPSV systems.

Remark 7 *Consider that* h_{p} *is very small such that* $\gamma = 1$. *Then, for sufficiently small N,* $1/(16N^4) \gg h_{\mathrm{p}}^2/N^2$ *such that the singular value scales quadratically. However, if* $N \geq 1/(4h_{\mathrm{p}})$. *the second term in the square root in* (10) *becomes dominant and the scaling improves to linear.*

These results are also verified numerically. The scaling of $\sigma_{\min}\left(\mathcal{B} + h_{\mathrm{p}}\langle\mathcal{B}\rangle\right)R\mathcal{B}^{\mathrm{T}}$ is shown in Fig. 2. It is clear that for SPAV $\sigma_{\min}$ scales with rate $1/N$, while for SPSV $\sigma_{\min}$

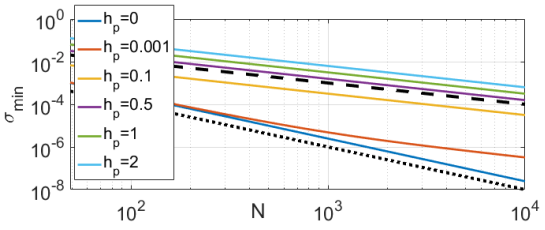

Figure 2. Scaling of $\sigma_{\min}\left(\left(\mathcal{B} + h_{\mathrm{p}}\langle\mathcal{B}\rangle\right)R\mathcal{B}^{\mathrm{T}}\right)$ for $R = I$ as a function of N with $h_{\mathrm{p}} = 0$ (SPSV) and various $h_{\mathrm{p}} > 0$ (SPAV). The dotted line is $1/N^2$ and the dashed line is $1/N$.

approaches zero faster, i. e., as $1/N^2$. The larger the asymmetry (greater h_{p}), the larger also the smallest singular value. Also, for very small asymmetry $h_{\mathrm{p}} = 0.001$, the scaling is quadratic for small N, and improves to linear for $N > 250$.

Remark 8 *Lemma 5 together with Fig. 2 suggest that* $\sigma_{\min}((\mathcal{B} + \tilde{\mathcal{B}}_{\mathrm{p}})R\mathcal{B}^{\mathrm{T}})$ *increases with* h_{p}, *leading to smaller deviation bounds and faster convergence rates. Although this is mathematically true, a practical implementation with* $h_{\mathrm{p}} > 1$ *might be fragile as the coupling of vehicle i with* $i+1$ *gets a positive sign, causing a locally positive feedback.* $h_{\mathrm{p}} \gg 1$ *also leads to high gains and potential actuator saturation. Thus, setting* $h_{\mathrm{p}} \leq 1$ *is preferable.*

4 Asymmetric position coupling

In this section, we allow asymmetric position coupling, i.e., $h_\Delta \geq 0$, and distinguish between $h_\Delta \leq h_{\mathrm{p}}$ and $h_\Delta > h_{\mathrm{p}}$.

4.1 Asymmetry in position less than in velocity, $h_\Delta \leq h_{\mathrm{p}}$

For $h_\Delta < 1$, the platoon can be modelled as

$$\begin{bmatrix}\dot{p}(t)\\ \dot{\Delta}(t)\end{bmatrix} = \begin{bmatrix} -\left(\mathcal{B}+\tilde{\mathcal{B}}_{\mathrm{p}}\right)R\mathcal{B}^{\mathrm{T}}E^{-1} & \frac{1}{1+h_\Delta}(\mathcal{B}+\tilde{\mathcal{B}}_\Delta)E^{-1} \\ -\mathcal{B}^{\mathrm{T}}E^{-1} & 0 \end{bmatrix} \nabla H_\Delta + \begin{bmatrix} d(t) \\ 0 \end{bmatrix}. \tag{13}$$

where

$$\begin{aligned} H_\Delta(p,\Delta) = & \frac{1}{2}(p(t) - M\underline{1}v_0)^{\mathrm{T}} E M^{-1}(p(t) - M\underline{1}v_0) \\ & + \frac{1}{2}\Delta^{\mathrm{T}}(t)(1+h_\Delta)EA\Delta(t). \end{aligned} \tag{14}$$

with the scaling matrix $E = \mathrm{diag}\left(1, \frac{1-h_\Delta}{1+h_\Delta}, \ldots, \left(\frac{1-h_\Delta}{1+h_\Delta}\right)^{N-1}\right)$.

Then, in Appendix C we prove the following properties.

Theorem 9 (APAV) *Consider system* (13) *under Assumptions 2 and 3 with Hamiltonian* (14). *Then,*

(i) the equilibrium (6) *of the autonomous system is asymptotically stable for* $h_{\mathrm{p}} \geq h_\Delta$ *and* $h_\Delta < 1$, *and*

(ii) the effect of disturbances is bounded as

$$H_\Delta(t) \leq H_\Delta(0) + \frac{\|d(\cdot)\|_2^2}{2\sigma_{\min}\left(E\left(\mathcal{B}+\tilde{\mathcal{B}}_{\mathrm{p}}\right)R\mathcal{B}^{\mathrm{T}}\right)}, \tag{15}$$

and $\sigma_{\min}\left(E\left(\mathcal{B}+\tilde{\mathcal{B}}_{\mathrm{p}}\right)R\mathcal{B}^{\mathrm{T}}\right)$ *for N sufficiently large approaches zero with rate* $1/c^N$, *with* $c > 1$.

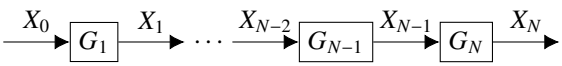

Figure 3. String model using the transfer function description $X_i(s) = G_i(s)X_{i-1}(s)$ with (16)-(17).

Remark 10 *Theorem 9 shows that the upper bound on the effect of the disturbance scales exponentially with N, which is much worse than the scaling for symmetric position coupling. Although this does not mean that the system does not scale better, the results in the literature confirm that at least for $h_p = h_\Delta$ the $\mathcal{H}_\infty$ norm of the transfer function scales exponentially with the graph distance, Herman, Martinec, Hurák & Sebek (2016). Similar results appeared in Seiler et al. (2004), Tangerman et al. (2012), Herman et al. (2015).*

Remark 11 *For the transition between APAV and SPAV or SPSV consider h_Δ to be very small and N sufficiently low. Then, the scaling matrix $E \approx I$, $\sigma_{\min}(E) \approx 1$, $H_\Delta \approx H$, and (15) becomes (7). Thus, the scaling is similar to the scaling of SPAV or SPSV, depending on h_p. But for large N, the scaling becomes exponential.*

4.2 Asymmetry in position greater than in velocity, $h_\Delta > h_p$

It will be shown that even short strings of length $N = 2$ become unstable for particular combinations of h_p and h_Δ. For simplicity, set $R = A = M = I$ and $\delta_{\text{ref}} = 0$. Then, applying the Laplace transform to the simplified state space equations (1), (2) and denoting $X_i(s) = \mathcal{L}\{x_i(t)\} = X_i$, yields

$$X_i = \underbrace{\frac{(1+h_p)s+(1+h_\Delta)}{s^2+2s+2}}_{:=G^-} X_{i-1} + \underbrace{\frac{(1-h_p)s+(1-h_\Delta)}{s^2+2s+2}}_{:=G^+} X_{i+1} \quad (16)$$

$$X_N = \underbrace{\frac{(1+h_p)s+(1+h_\Delta)}{s^2+(1+h_p)s+1+h_\Delta}}_{:=G_N} X_{N-1}. \quad (17)$$

By writing $X_i(s) = G_i(s)X_{i-1}(s)$, the transfer functions G_i for $i < N$ can be derived recursively using the relation $G_i = (1-G^+G_{i+1})^{-1}G^-$ such that the dynamics of the entire string can be described as illustrated in Fig. 3. Then, it can be shown that some strings of length $N = 2$ are unstable:

Lemma 12 *Strings of $N \geq 2$ vehicles are unstable if $h_\Delta \geq \frac{2h_p^4+12h_p^3+25h_p^2+30h_p+11}{3h_p^2+6h_p+7}$ or $h_\Delta \geq \frac{h_p^3+5h_p^2+8h_p+10}{h_p-1}$ for $h_p > 1$.*

PROOF. The results in (16) and (17) and tedious calculations reveal that the denominator of G_{N-1} is $s^4+(3+h_p)s^3+(3+h_\Delta+(1+h_p)^2)s^2+2(1+h_p)(1+h_\Delta)s+(1+h_\Delta)^2$. Using the Hurwitz stability criterion, and considering $h_p, h_\Delta \geq 0$, the result follows. Hence, if those bounds are violated, then the second last transfer function in the string is unstable, yielding an unstable string. □

Fig. 4 shows the maximal stable string length $\bar{N}_{\text{stab}}$ for combinations of h_p and h_Δ. It can be seen that longer strings remain stable for smaller ratios h_Δ/h_p. Also, from Theorem 9 it follows that strings of arbitrary lengths are stable if $h_\Delta \leq h_p$ and $h_\Delta < 1$ (the border is marked with a red line). Based on those observations, we conjecture:

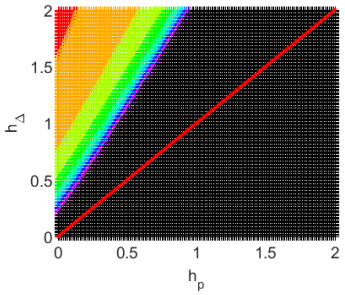

Figure 4. Maximal stable string length $\bar{N}_{\text{stab}}$ as a function of h_p and h_Δ: $\bar{N}_{\text{stab}} = 1$ in red, $\bar{N}_{\text{stab}} = 2$ in orange, ..., $\bar{N}_{\text{stab}} = 10$ in purple, $\bar{N}_{\text{stab}} > 10$ in black

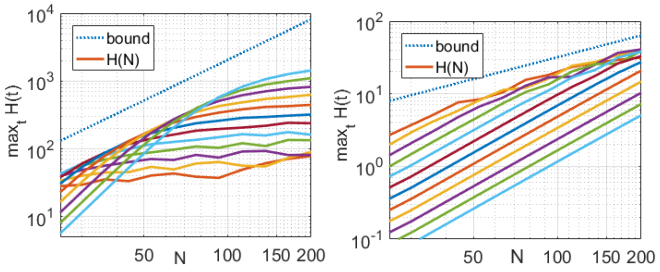

(a) SPSV (b) SPAV

Figure 5. Plot of maximal value of $H(t)$ for SPSV and SPAV when the input is applied for different times ($T_f \in [200, 10000]$) and $N = 25, \ldots, 200$. The dashed line is the bound (7).

Conjecture 13 *For every $h_\Delta > h_p$ there exists a maximal string length $\bar{N}_{\text{stab}}$ for which the system is stable and all strings of length $N > \bar{N}_{\text{stab}}$ are unstable.*

5 Examples and simulations

First, simulations confirming the quadratic and linear growth are discussed. The disturbance is chosen parallel to $p(t)$ to achieve the fastest growth of the energy, i.e., $d_i(t) = p_i(t)/\left(\|p\|_2\sqrt{T_f}\right)$ for $t < T_f$ and $d_i(t) = 0$ for $t > T_f$, such that $\|d(\cdot)\|_2 = 1$ for all N. The initial conditions are zero in all simulations. We are interested in the maximal value of the Hamiltonian functions $H_{\max} = \max_t H(p(t), \Delta(t))$.

First consider SPSV. Different durations of the input signal in the range $T_f \in [200, 10000]$ were used, see Fig. 5a, where the solid lines correspond to different T_f. The longer T_f is chosen, the lower the value for low N and the higher the maximal value of H become. On the curve for each T_f, consider the point which is the closest to the bound. From the plot in Fig. 5a it is apparent that this point scales quadratically with N. The illustration of the SPAV case in Fig. 5b shows that the growth of the point, where each curve gets closest to the bound, is linear. Also note that, for a given N, $\max_t H(t)$ is much smaller for SPAV, than for SPSV. The bounds are conservative but capture the scaling qualitatively.

To investigate the transients, assume zero initial states and $x_0 = t$. Further, $r_i = a_i = m_i = 1, \delta_{\text{ref}\,i-1,i} = 0\,\forall i$, in SPAV $h_p = 0.5\,\forall i$ and in APAV $h_p = 0.5, h_\Delta = 0.2, \forall i$.

The time-domain plots in Fig. 6 show that SPAV has shorter convergence time and lower overshoots than SPSV.

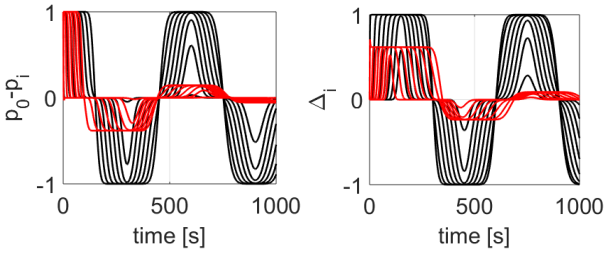

(a) Momentum SPSV, SPAV (b) Pos. error SPSV, SPAV

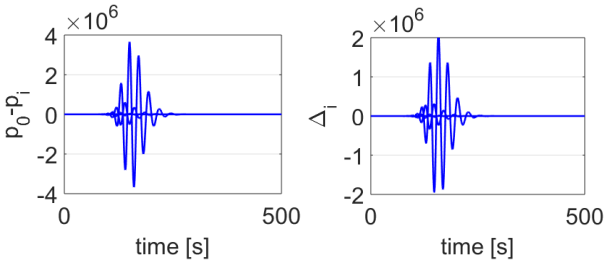

(c) Momentum APAV (d) Pos. error APAV

Figure 6. Response of the platoon with $N = 150$ to the leader's step change in velocity. Black is SPSV, red is SPAV, blue is APAV.

When asymmetry in position is introduced (APAV), extremely high peaks occur. Despite the fact that the leader moves with unit velocity, during the transient the states of some vehicles reached up to the order of 10^6. Such large peaks imply that, especially for larger platoons, APAV should not be used in practical application. It might be a reasonable solution only for small platoons.

The scaling of other quantities in Fig 7, shows:

- *Maximal overshoot* $\max_{i,t} \Delta_i(N,t)$ (Fig. 7a): Both SPSV and SPAV are bounded for all N, while SPAV achieves a lower bound. APAV scales exponentially.
- *Maximal control effort* $\max_{i,t} F_i(t)$ (Fig. 7b): The control effort of SPSV and SPAV does not grow with N, while it scales exponentially for APAV.
- *Convergence time* (Fig. 7c): SPAV and APAV scale linearly, while SPSV scales quadratically with N.
- *Total error* $E = \sum_{i=1}^{N} \int_0^\infty \Delta_i^2 + (v_i - v_0)^2 dt$. (Fig. 7d): SPAV achieves quadratic scaling, SPSV scales cubically and APAV scales again exponentially with N.

Hence, SPAV outperforms SPSV and APAV in all cases apart from the convergence time. It is true that APAV achieved about 4 times faster transient, but at the price of exponential scaling of any other quantity.

6 Summary and discussion

Now we summarize our results in terms of the disturbance scaling in Def. 1. Define two vectors of deviation from the equilibrium (6):

$$\chi_{\mathrm{p}} = \sqrt{1/2}\,\mathrm{col}\Big(M^{-1/2}(p(t) - M\underline{1}v_0), A^{1/2}\Delta\Big), \tag{18}$$

$$\chi_{\Delta} = \sqrt{1/2}\,\mathrm{col}\Big((EM)^{-1/2}(p(t) - M\underline{1}v_0), (1+h_{\Delta})^{1/2}E^{1/2}A^{1/2}\Delta\Big). \tag{19}$$

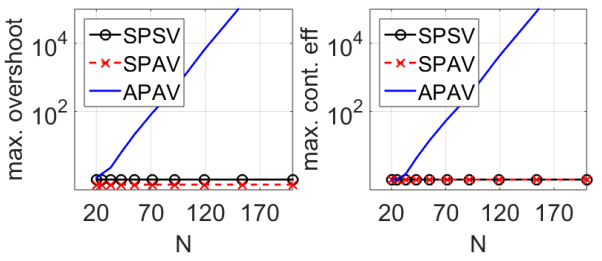

(a) Max. overshoot (b) Max. cont. eff.

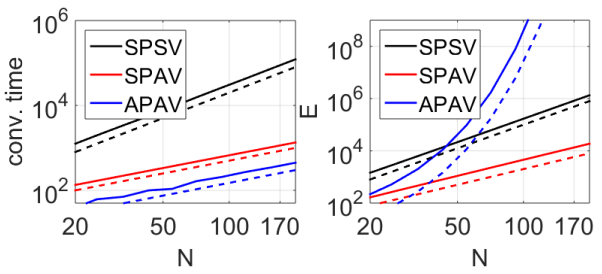

(c) Conv. time (d) Total error

Figure 7. Scaling of quantities of interest for $x_0 = t$. Note that a) and b) are in semilogarithmic coordinates, c) and d) in logarithmic coordinates. The dashed lines are in c) $2N^2$ (black), $5N$ (red) and $1.5N$ (blue) and in d) $0.1N^3$ (black), $0.2N^2$ (red) and $e^{0.17N}$ (blue).

Then $H = \chi_{\mathrm{p}}^{\mathrm{T}}\chi_{\mathrm{p}} = \|\chi_{\mathrm{p}}\|_2^2$ and $H_{\Delta} = \chi_{\Delta}^{\mathrm{T}}\chi_{\Delta} = \|\chi_{\Delta}\|_2^2$. Hence, the scaling of the Hamiltonians directly relates to the disturbace scaling. The main results of this paper are summarised in the following theorem.

Theorem 14 *The qualitative effect of the disturbance on the deviations from the equilibrium scales with the number of vehicles N as*

- *(SPSV):* $\|\chi_{\mathrm{p}}(t)\|_2^2 \le \|\chi_{\mathrm{p}}(0)\|_2^2 + \|d(\cdot)\|_2^2 \frac{1}{c_1} N^2$.
- *(SPAV):* $\|\chi_{\mathrm{p}}(t)\|_2^2 \le \|\chi_{\mathrm{p}}(0)\|_2^2 + \|d(\cdot)\|_2^2 \frac{1}{c_2} N$.
- *(APAV):* $\|\chi_{\Delta}(t)\|_2^2 \le \|\chi_{\Delta}(0)\|_2^2 + \|d(\cdot)\|_2^2 \frac{1}{c_3} c^N$. *This holds for $h_{\mathrm{p}} \ge h_{\Delta}$ and $h_{\Delta} < 1$.*

where $c_1, c_2, c_3 > 0$ and $c > 1$ are some constants independent of N. For $h_{\Delta} > h_{\mathrm{p}}$ we conjecture instability for a sufficiently large string length N.

PROOF. The scaling for SPSV and SPAV follows from (12) and (11), respectively, in (7). Scaling of APAV directly follows from Theorem 9. The conjecture about instability is based on Lemma 12 and numerical simulations. □

The results of Theorem 14 are illustrated in Fig. 1. For symmetric coupling in position and asymmetric in velocity (SPAV, case A) it was shown that the scaling is linear in N. When the coupling becomes symmetric also in velocity (SPSV, case B) the scaling deteriorates to N^2. If the asymmetry in position is less than the asymmetry in velocity (APAV, case C), the scaling is exponential in the worst case. We conjecture, based on numerical simulations, that the exponential scaling also occurs in case D. In the region E, there exist combinations of h_{Δ} and h_{p} for which even

trivial strings of length $N = 2$ are unstable. We conjecture that for all $h_\Delta > h_\mathrm{p}$ there exists a critical stable string length beyond which the string becomes unstable.

Scaling in some of the regions were known previously. For instance, the case $h_\mathrm{p} = h_\Delta = 1$ corresponds to the predecessor following (PF) case, for which Seiler et al. (2004) proved that the $\mathcal{H}_\infty$ norm grows exponentially. Later, this was generalised in Tangerman et al. (2012), Herman et al. (2015) to $0 \leq h_\mathrm{p} = h_\Delta \leq 1$. However, these popular choices are clearly outperformed by choosing $h_\mathrm{p} > 0$ and $h_\Delta = 0$ (case A). This effect is also illustrated by several numerical simulations discussed above. Therefore, we believe that the results presented in this paper should lead to a new "standard", that is, choosing $h_\mathrm{p} > 0$ and $h_\Delta = 0$.

Symmetric velocity coupling can be interpreted as virtual dampers, whereas symmetric position couping can be seen as virtual springs. The dampers are instances of generalised resistances, Jeltsema & Scherpen (2009), which extract energy from the system. When introducing asymmetric dampers, only *how* the energy is extracted is changed. Allowing asymmetric position coupling has a different effect: Assuming ideal springs, a force acting on one side of the spring is exactly the opposite of a force at the other side of the spring by Newton's third law. This fundamental law is violated when introducing asymmetric position coupling: Consider $A = I$, $\Delta_i > 0$ and $h_\Delta > 0$. Then, the force, which is pulling the preceding vehicle backwards, is $(1 - h_\Delta)\Delta_i$, while the force, which is pulling the following vehicle forward, is $(1+h_\Delta)\Delta_i$. Combining them yields $2h_\Delta\Delta_i > 0$. Thus, asymmetric position coupling introduces additional forces, and hence adds energy to the system.

A Proof of Lemma 5

First, consider the symmetric case such that $\left(\mathcal{B} + \tilde{\mathcal{B}}_\mathrm{p}\right) R\mathcal{B}^\mathrm{T} = \mathcal{B}R\mathcal{B}^\mathrm{T}$. Let $D = R^{1/2}$. Then $\mathcal{B}R\mathcal{B}^\mathrm{T} = (\mathcal{B}D)(\mathcal{B}D)^T$ and $\sigma_{\min}(\mathcal{B}D) \geq \sqrt{\underline{r}}\sigma_{\min}(\mathcal{B})$ (Bernstein 2009, Prop. 9.6.4). Then the minimal singular value (= minimal eigenvalue) can be bounded by $\lambda_{\min}\left(\mathcal{B}R\mathcal{B}^\mathrm{T}\right) \geq \underline{r}\lambda_{\min}\left(\mathcal{B}\mathcal{B}^\mathrm{T}\right)$, with $\mathcal{B}\mathcal{B}^\mathrm{T}$ being a pinned Laplacian for an undirected path graph. Its eigenvalues are given as (Parlangeli & Notarstefano 2012, Prop. 3.3) $\lambda_i = 2\left(1 - \cos\frac{(2i-1)\pi}{2N+1}\right) = 4\sin^2\frac{(2i-1)\pi}{4N+2}$, $i = 1, \ldots, N$. The smallest eigenvalue λ_1 is bounded using $\sin x \geq 2x/\pi$ as

$$\lambda_1(\mathcal{B}\mathcal{B}^\mathrm{T}) = 4\sin^2\frac{\pi}{4N+2} \geq 4\frac{1}{(2N+1)^2} \geq \frac{1}{4}\frac{1}{N^2}. \quad \text{(A.1)}$$

Then we get the quadratic bound

$$\lambda_{\min}\mathcal{B}R\mathcal{B}^\mathrm{T} \geq \underline{r}\, 1/(4N^2). \quad \text{(A.2)}$$

Denote $L_p = (\mathcal{B}+h_\mathrm{p}\langle\mathcal{B}\rangle)R\mathcal{B}^\mathrm{T}$. Then, $\sigma^2_{\min}\left((\mathcal{B} + h_\mathrm{p}\langle\mathcal{B}\rangle)R\mathcal{B}^\mathrm{T}\right) = \lambda_{\min}\left({L_p}^\mathrm{T}L_p\right) = \lambda_{\min}\Big[(\mathcal{B}R\mathcal{B}^\mathrm{T})^\mathrm{T}(\mathcal{B}R\mathcal{B}^\mathrm{T}) + h_\mathrm{p}^2\mathcal{B}R\langle\mathcal{B}\rangle^\mathrm{T}\langle\mathcal{B}\rangle R\mathcal{B}^\mathrm{T} + h_\mathrm{p}\left(\mathcal{B}R\left(\langle\mathcal{B}\rangle^\mathrm{T}\mathcal{B} + \mathcal{B}^\mathrm{T}\langle\mathcal{B}\rangle\right)R\mathcal{B}^\mathrm{T}\right)\Big] \geq \underline{r}^2\lambda_{\min}\left(\Gamma_1 + h_\mathrm{p}\Gamma_2 + h_\mathrm{p}^2\Gamma_3\right)$ with $\Gamma_1 = (\mathcal{B}\mathcal{B}^\mathrm{T})^\mathrm{T}(\mathcal{B}\mathcal{B}^\mathrm{T})$, $\Gamma_2 = \left(\mathcal{B}\left(\langle\mathcal{B}\rangle^\mathrm{T}\mathcal{B} + \mathcal{B}^\mathrm{T}\langle\mathcal{B}\rangle\right)\mathcal{B}^\mathrm{T}\right) = \mathrm{diag}(2, 0, .., 0)$ and $\Gamma_3 = \mathcal{B}\langle\mathcal{B}\rangle^\mathrm{T}\langle\mathcal{B}\rangle\mathcal{B}^\mathrm{T}$. Restructuring yields $\lambda_{\min}\left({L_p}^\mathrm{T}L_p\right) \geq \underline{r}^2\lambda_{\min}\left(\Gamma_1 + h_\mathrm{p}^2\Psi_1 + h_\mathrm{p}^2\Psi_2\right)$, where

$$\Psi_1 = \begin{bmatrix} 1+\frac{2}{h_\mathrm{p}} & 0 & -1 & 0 & 0 & \ldots & 0 \\ 0 & 2 & 0 & -1 & 0 & \ldots & 0 \\ -1 & 0 & 2 & 0 & -1 & \ddots & \vdots \\ 0 & \ddots & \ddots & \ddots & \ddots & \ddots & 0 \\ \vdots & \ddots & -1 & 0 & 2 & 0 & -1 \\ 0 & \ldots & 0 & -1 & 0 & 1 & 0 \\ 0 & \ldots & 0 & 0 & -1 & 0 & 1 \end{bmatrix} \quad \text{(A.3)}$$

and Ψ_2 is a matrix of zeros with $\begin{bmatrix} 1 & -1 \\ -1 & 1 \end{bmatrix}$ in the bottom-right corner. Using (Bernstein 2009, Fact 5.12.2) yields

$$\lambda_{\min}\left({L_p}^\mathrm{T}L_p\right) \geq \underline{r}^2\left(\lambda_{\min}\Gamma_1 + h_\mathrm{p}^2\lambda_{\min}(\Psi_1) + h_\mathrm{p}^2\lambda_{\min}(\Psi_2)\right). \quad \text{(A.4)}$$

By (A.1), $\lambda_{\min}(\Gamma_1) = \lambda_{\min}(\mathcal{B}\mathcal{B}^\mathrm{T})^2 \geq 1/(16N^4)$. The matrix Ψ_2 is positive semi-definite matrix, hence $\lambda_{\min}(\Psi_2) = 0$. It remains to investigate $\lambda_{\min}(\Psi_1)$. Note that Ψ_1 is a reducible matrix. Using the permutation matrix $P = [\vec{e}_1, \vec{e}_3, \ldots \vec{e}_{N-1}, \vec{e}_2, \vec{e}_4, \ldots \vec{e}_N]$, leads to $\lambda_{\min}(\Psi_1) = \lambda_{\min}\left(P^{-1}\Psi_1 P\right) = \lambda_{\min}\left(\begin{bmatrix} L_1 & 0 \\ 0 & L_2 \end{bmatrix}\right)$, with $L_1 = \bar{\mathcal{B}}D\bar{\mathcal{B}}^\mathrm{T}$, $L_2 = \bar{\mathcal{B}}\bar{\mathcal{B}}^\mathrm{T}$ where $D = \mathrm{diag}(1/h_\mathrm{p}, 1, \ldots, 1)$ and $\bar{\mathcal{B}}$ has the same structure as $\mathcal{B}$ but half the size. It follows that $\lambda_{\min}(\Psi_1) = \min\{\lambda_{\min}(L_1), \lambda_{\min}(L_2)\}$. Let $\gamma = \min\{1/h_\mathrm{p}, 1\}$. Then $\lambda_{\min}(L_1) \geq \gamma\lambda_{\min}\bar{\mathcal{B}}\bar{\mathcal{B}}^\mathrm{T}$ and $\lambda_{\min}(L_2) = \lambda_{\min}\left(\bar{\mathcal{B}}\bar{\mathcal{B}}^\mathrm{T}\right)$. Hence, $\lambda_{\min}(\Psi_1) \geq \gamma\lambda_{\min}\left(\bar{\mathcal{B}}\bar{\mathcal{B}}^\mathrm{T}\right)$. Since $\bar{\mathcal{B}} \in \mathrm{R}^{N/2\times N/2}$, from (A.1) we get $\lambda_{\min}(\Psi_1) \geq \gamma/N^2$. Using this, (A.1), (A.4) and $\lambda_{\min}(\Psi_2) = 0$ yields (10).

B Proof of Lemma 6

The lower bound is given by (10). For $h_\mathrm{p} = 0$, quadratic scaling is shown in (A.2). For $h_\mathrm{p} > 0$, the approach with rate $1/N^4$ is much faster than the approach of $h_\mathrm{p}^2\gamma/N^2$, hence for N sufficiently large $\sigma_{\min}((\mathcal{B} + \tilde{\mathcal{B}}_\mathrm{p})R\mathcal{B}) \geq \underline{r}h_\mathrm{p}\sqrt{\gamma}/N$. For the upper bound, note that $\sigma_{\min}\left(\left(\mathcal{B} + \tilde{\mathcal{B}}_\mathrm{p}\right)R\mathcal{B}^\mathrm{T}\right) \leq \bar{r}\sigma_{\min}\left(\left(\mathcal{B} + \tilde{\mathcal{B}}_\mathrm{p}\right)\mathcal{B}^\mathrm{T}\right)$, where $\left(\mathcal{B} + \tilde{\mathcal{B}}_\mathrm{p}\right)\mathcal{B}^\mathrm{T}$ has the form

$$\begin{bmatrix} 2 & -(1-h_\mathrm{p}) & 0 & \ldots & 0 \\ -(1+h_\mathrm{p}) & 2 & -(1-h_\mathrm{p}) & \ldots & 0 \\ \vdots & \vdots & \vdots & \ddots & \vdots \\ 0 & \ldots & -(1+h_\mathrm{p}) & 2 & -(1-h_\mathrm{p}) \\ 0 & \ldots & 0 & -(1+h_\mathrm{p}) & 1+h_\mathrm{p} \end{bmatrix}. \quad \text{(B.1)}$$

As its leading principal submatrix of size $N-1$, it has a finite Toeplitz matrix, denoted as M_N. The matrix M_N has as its symbol $a(t) = -(1 - h_\mathrm{p})t^{-1} + 2 - (1 + h_\mathrm{p})t^1$ with $t \in \mathbb{C}, |t| = 1$. The symbol is not Fredholm, because it has a zero at $t = 1$. The order α of the zero at $t = 1$ is either 1 for $h_\mathrm{p} > 0$ or 2 for $h_\mathrm{p} = 0$. The result (Böttcher & Grudsky 2005, Thm. 9.8) specifies scaling of singular values for Toeplitz matrices as $\sigma_i(M_N) = O\left(1/N^\alpha\right)$ for any fixed i with

$\sigma_i \leq \sigma_{i+1}$. That is, the singular values go to zero with a rate at least given by the order of the zero of the symbol. Since M_N is a submartix of $\left(\mathcal{B}+\tilde{\mathcal{B}}_\mathrm{p}\right)\mathcal{B}^\mathrm{T}$, by (Böttcher & Grudsky 2005, Thm. 9.7) it follows $\sigma_{\min}\left(\left(\mathcal{B}+\tilde{\mathcal{B}}_\mathrm{p}\right)\mathcal{B}^\mathrm{T}\right) \leq \sigma_3(M_N)$. Then, $\sigma_3(M_N) = O(1/N^\alpha)$, and hence $\sigma_3(M_N) \leq c/N^\alpha$. Thus, $\sigma_{\min}\left(\left(\mathcal{B}+\tilde{\mathcal{B}}_\mathrm{p}\right)\mathcal{B}^\mathrm{T}\right) \leq c_2/N$ if $h_\mathrm{p} > 0$ and $\sigma_{\min}\left(\left(\mathcal{B}+\tilde{\mathcal{B}}_\mathrm{p}\right)\mathcal{B}^\mathrm{T}\right) \leq c_4/N^2$ if $h_\mathrm{p} = 0$. □

C Proof of Theorem 9

First we show that (13) is a skew-symmetric form. It can be verified that $\left(\frac{1}{1+h_\Delta}\mathcal{B} + \frac{h_\Delta}{1+h_\Delta}\langle\mathcal{B}\rangle\right) = I - \frac{1-h_\Delta}{1+h_\Delta}D_\mathrm{u}$, where D_u has ones only at the first upper-diagonal. Also, $\frac{1-h_\Delta}{1+h_\Delta}D_\mathrm{u}E^{-1} = E^{-1}D_\mathrm{u}$. This yields $\left(\frac{1}{1+h_\Delta}\mathcal{B} + \frac{h_\Delta}{1+h_\Delta}\langle\mathcal{B}\rangle\right)E^{-1} = (I-\frac{1-h_\Delta}{1+h_\Delta}D_\mathrm{u})E^{-1} = E^{-1} - E^{-1}D_\mathrm{u} = E^{-1}\mathcal{B} = -(-\tilde{\mathcal{B}}E^{-1})^\mathrm{T}$.

(i) Use H_Δ in (14) as a Lyapunov function and set $d(t) = 0$. With $\tilde{v} := M^{-1}(p - M\underline{1}v_0)$ such that $\nabla_\mathrm{p}H_\Delta = E\tilde{v}$, the time derivative is $\dot{H}_\Delta = -\tilde{v}^\mathrm{T}E\left(\mathcal{B}+\tilde{\mathcal{B}}_\mathrm{p}\right)R\mathcal{B}^\mathrm{T}\tilde{v}$. This is equivalent to $-\tilde{v}^\mathrm{T}S\tilde{v}$ with $S = \frac{1}{2}\left(E\left(\mathcal{B}+\tilde{\mathcal{B}}_\mathrm{p}\right)R\mathcal{B}^\mathrm{T} + \mathcal{B}R(\mathcal{B}+\tilde{\mathcal{B}}_\mathrm{p})^\mathrm{T}E\right)$, $S = S^\mathrm{T}$. Thus, $-\tilde{v}^\mathrm{T}E\left(\mathcal{B}+\tilde{\mathcal{B}}_\mathrm{p}\right)R\mathcal{B}^\mathrm{T}\tilde{v} < 0$ for all $\tilde{v}$ if and only if $S > 0$. The sum s_i of the ith row of S is $s_i = \left((h_\mathrm{p}-h_\Delta)(r_i(1+h_\Delta) - r_{i+1}(1-h_\Delta))(1-h_\Delta)^{i-2}\right)/(1+h_\Delta)^i$ and the sums $s_1 = \left((1+h_\Delta+h_\mathrm{p}+h_\Delta h_\mathrm{p})r_1 - r_2(h_\mathrm{p}-h_\Delta)\right)/\left(1+h_\Delta\right)$ and $s_N = r_N((h_\mathrm{p}-h_\Delta)(1-h_\Delta)^{N-2})/(1+h_\Delta)^{N-1}$. Recall that by Assumption 3 $r_i \geq r_{i+1}$. Then if $h_\mathrm{p} > h_\Delta$ and $h_\Delta < 1$, all sums s_i are positive, so $S > 0$. Then, $\dot{H}_\Delta \leq 0$ and the invariance principle completes the proof. For $h_\mathrm{p} = h_\Delta < 1$ see (Tangerman et al. 2012, Thm 2.3).

(ii) Consider $d(t) \neq 0$. The derivative of H_Δ is $\dot{H}_\Delta = -\tilde{v}^\mathrm{T}E(\mathcal{B}+\tilde{\mathcal{B}}_\mathrm{p})R\mathcal{B}^\mathrm{T}\tilde{v} + \tilde{v}^\mathrm{T}Ed$. It can be bounded since $\dot{H}_\Delta \leq -\sigma_{\min}\left(E\left(\mathcal{B}+\tilde{\mathcal{B}}_\mathrm{p}\right)R\mathcal{B}^\mathrm{T}\right)|\tilde{v}|^2 + \tilde{v}^\mathrm{T}Ed$. Completing the squares then leads to a similar form as in (9) such that $\dot{H}_\Delta \leq \frac{|Ed|_2^2}{2\sigma_{\min}\left(E\left(\mathcal{B}+\tilde{\mathcal{B}}_\mathrm{p}\right)R\mathcal{B}^\mathrm{T}\right)} \leq \frac{|d|_2^2}{2\sigma_{\min}\left(E\left(\mathcal{B}+\tilde{\mathcal{B}}_\mathrm{p}\right)R\mathcal{B}^\mathrm{T}\right)}$ since $\sigma_{\max}(E) = 1$. (15) follows from integration with respect to time. The smallest singular value of $E\left(\mathcal{B}+\tilde{\mathcal{B}}_\mathrm{p}\right)R\mathcal{B}^\mathrm{T}$ can be upper bounded as (Bernstein 2009, Prop. 9.6.6) $\sigma_{\min}\left(E\left(\mathcal{B}+\tilde{\mathcal{B}}_\mathrm{p}\right)R\mathcal{B}^\mathrm{T}\right) \leq \sigma_{\min}(E)\sigma_{\max}\left(\left(\mathcal{B}+\tilde{\mathcal{B}}_\mathrm{p}\right)R\mathcal{B}^\mathrm{T}\right)$. By Gershgorin's Theorem, $\sigma_{\max}\left(\left(\mathcal{B}+\tilde{\mathcal{B}}_\mathrm{p}\right)R\mathcal{B}^\mathrm{T}\right) \leq \bar{r}\sigma_{\max}((\mathcal{B}+\tilde{\mathcal{B}}_\mathrm{p})\mathcal{B}^\mathrm{T}) \leq 4\bar{r}$. Also, $\sigma_{\min}(E) = \left(\frac{1-h_\Delta}{1+h_\Delta}\right)^{N-1}$. Then, $\sigma_{\min}(E(\mathcal{B}+\tilde{\mathcal{B}}_\mathrm{p})R\mathcal{B}^\mathrm{T}) \leq \left(\frac{1-h_\Delta}{1+h_\Delta}\right)^{N-1}4\bar{r} \propto \frac{1}{c^N}$, with $c = \frac{1+h_\Delta}{1-h_\Delta} > 1$. Thus, $\sigma_{\min}\left(E\left(\mathcal{B}+\tilde{\mathcal{B}}_\mathrm{p}\right)R\mathcal{B}^\mathrm{T}\right)\Big)$ goes to zero exponentially fast. □

References

Alam, A., Mårtensson, J. & Johansson, K. H. (2015), 'Experimental evaluation of decentralized cooperative cruise control for heavy-duty vehicle platooning', *Control Engineering Practice* **38**.

Barooah, P. & Hespanha, J. (2005), Error Amplification and Disturbance Propagation in Vehicle Strings with Decentralized Linear Control, *in* '44th IEEE CDC', pp. 4964–4969.

Barooah, P., Mehta, P. & Hespanha, J. (2009), 'Mistuning-Based Control Design to Improve Closed-Loop Stability Margin of Vehicular Platoons', *IEEE Trans. Autom. Control* **54**(9).

Bernstein, D. (2009), *Matrix Mathematics*, Princeton Univ. Press.

Böttcher, A. & Grudsky, S. (2005), *Spectral Properties of Banded Toeplitz Matrices*, SIAM.

Cantos, C. E., Hammond, D. K. & Veerman, J. J. P. (2016), 'Transients in the synchronization of asymmetrically coupled oscillator arrays', *Eur. Phys. J.: Spec. Topics* **225**(6-7), 1199–1209.

Hao, H. & Barooah, P. (2010), 'Control of large 1D networks of double integrator agents: Role of heterogeneity and asymmetry on stability margin', *IEEE CDC* pp. 7395–7400.

Hao, H. & Barooah, P. (2012), 'Stability and robustness of large platoons of vehicles with double-integrator models and nearest neighbor interaction', *Intern. Journal of Robust and Nonlinear Control* **23**(8), 2097–2122.

Hao, H., Yin, H. & Kan, Z. (2012), On the robustness of large 1-D network of double integrator agents, *in* 'ACC', pp. 6059–6064.

Herman, I., Martinec, D., Hurák, Z. & Sebek, M. (2015), 'Nonzero Bound on Fiedler Eigenvalue Causes Exponential Growth of H-Infinity Norm of Vehicular Platoon', *IEEE Trans. Autom. Control* **60**(8), 2248–2253.

Herman, I., Martinec, D., Hurák, Z. & Sebek, M. (2016), 'Scaling in bidirectional platoons with dynamic controllers and proportional asymmetry', *IEEE Trans. Autom. Control* pp. 1–7.

Herman, I., Martinec, D. & Veerman, J. J. P. (2016), 'Transients of platoons with asymmetric and different Laplacians', *Systems & Control Letters* **91**, 28–35.

Jeltsema, D. & Scherpen, J. (2009), 'Multidomain modeling of nonlinear networks and systems', *IEEE Control Systems Magazine* **29**(4), 28–59.

Khalil, H. K. (2001), *Nonlinear Systems*, third edn, Prentice Hall.

Klinge, S. & Middleton, R. H. (2009), String stability analysis of homogeneous linear unidirectionally connected systems with nonzero initial conditions, *in* 'IET Irish Signals and Systems Conference'.

Knorn, S. & Ahlén, A. (2016), 'Deviation bounds in multi agent systems described by undirected graphs', *Automatica* **67**.

Knorn, S., Donaire, A., Agüero, J. C. & Middleton, R. H. (2015), 'Scalability of bidirectional vehicle strings with static and dynamic measurement errors', *Automatica* **62**, 208–212.

Knorn, S., Donaire, A., Agüero, J. & Middleton, R. (2014), 'Passivity-based control for multi-vehicle systems subject to string constraints', *Automatica* **50**(12), 3224–3230.

Martinec, D., Herman, I. & Sebek, M. (2016), 'On the necessity of symmetric positional coupling for string stability', *IEEE Trans. Autom. Control* .

Middleton, R. & Braslavsky, J. (2010), 'String Instability in Classes of Linear Time Invariant Formation Control With Limited Communication Range', *IEEE Trans. Autom. Control* .

Parlangeli, G. & Notarstefano, G. (2012), 'On the Reachability and Observability of Path and Cycle Graphs', *IEEE Trans. Autom. Control* **57**(3), 743–748.

Ploeg, J., van de Wouw, N. & Nijmeijer, H. (2014), 'Lp String Stability of Cascaded Systems: Application to Vehicle Platooning', *IEEE Transactions on Control Systems Technology* **22**(2).

Seiler, P., Pant, A. & Hedrick, K. (2004), 'Disturbance propagation in vehicle strings', *IEEE Trans. Autom. Control* **49**(10).

Tangerman, F., Veerman, J. & Stosic, B. (2012), 'Asymmetric decentralized flocks', *IEEE Trans. Autom. Control* **57**(11).

Veerman, J., Stosic, B. & Olvera, A. (2007), 'Spatial instabilities and size limitations of flocks', *Networks and Heterog. Media* **2**(4).